Micron 92 (2017) 13–18

Contents lists available at ScienceDirect

Micron

journal homepage: www.elsevier.com/locate/micron

# In situ tracking the reversible spinel-rocksalt structural transformation between $Mn_3O_4$ and MnO

Xingyuan San, Bo Zhang*, Jing Wang, Bo Wu, Xiuliang Ma

*Shenyang National Laboratory for Materials Science, Institute of Metal Research, Chinese Academy of Sciences, Wenhua Road 72, 110016 Shenyang, China*

ARTICLE INFO

*Article history:*
Received 29 July 2016
Received in revised form
18 September 2016
Accepted 18 September 2016
Available online 27 October 2016

*Keywords:*
In-situ transmission electron microscopy
$Mn_3O_4$
Reversible transformation
Beam irradiation

ABSTRACT

Electron beam irradiation is well known to induce damage in materials. The structural transformation involved in the damage is usually believed to be an irreversible solid state chemical reaction. Here we use in situ transmission electron microscopy (TEM) combined electron-energy loss spectroscopy (EELS) technique in an aberration-corrected TEM to track the structural transformation in spinel $Mn_3O_4$ induced by electron beam irradiation. It is clarified that spinel $Mn_3O_4$ is transformed to rocksalt structured MnO by irradiation and the reversed recovering transition from rocksalt MnO to spinel $Mn_3O_4$ can occur by aging in the gentle electron beam circumstance. The mechanisms including the role of O desorption/adsorption and the displacement of Mn and O involved in the reversible transformation processes are discussed. The work presents an implication that electron beam can modify the structure at atomic dimension yielding diverse assemblies of surfaces, interfaces and colorful properties.

## 1. Introduction

The $AB_2O_4$ spinel structures exhibit unusual physical, chemical and rheological properties (Radaelli et al., 2002; Liang et al., 2011; Karato et al., 1998), thus attracting much attention from the scientific community for many years. In spinel transition metal oxides, $Mn_3O_4$, due to its low-cost, environmental benignity, and unusual property, is a good candidate as pervasive application material (Seo et al., 2004; Wang et al., 2010; Li et al., 2014). The refined structure of $Mn_3O_4$ has been intensively studied experimentally, especially the oxidation states of Mn in the distorted spinel structure of $Mn_3O_4$ (Xiao et al., 2004; Tan et al., 2011). Of particular importance the atomic resolution elemental mapping has become feasible over the past years by means of spatially resolved electron-energy loss spectroscopy (EELS) with high-angle annular dark field (HAADF) technique in an aberration-corrected electron microscope (Tan et al., 2011; Yu et al., 2010). However, the manganese oxide compound has found to be extremely sensitive to damage by the electron beam in the transmission electron microscopy (TEM), especially in the STEM-EELS experiments performed at 300 kV. The behavior of manganese oxide compounds under electron beams is also important for energy application (Phillips et al., 2014; Lin et al., 2014). Previous studies paid little attention on the reversible transformation of manganese oxide compounds (Phillips et al., 2014; Lin et al., 2014), even believed the transformation induced by the electron beam irradiation is an irreversible solid state chemical reaction (Pennycook et al., 2014). Here, we report an interesting reversible spinel-rocksalt structural phase transition between $Mn_3O_4$ and MnO under electron irradiation.

## 2. Experimental

The well-shaped spinel $Mn_3O_4$ nano-octahedral particles were prepared by the hydrothermal method (Li et al., 2011). A drop of the solution containing the $Mn_3O_4$ powders was dripped on holey carbon films which supported on a copper mesh grid, then dried for further TEM observation. The TEM specimen was observed initially and recorded the original structural feature. Then the electron beam was focused to irradiate the small edge region with the electron flux of near $9 \times 10^5$ A/m$^2$. During the irradiating process, the beam-induced structural evolution was monitored and recorded. Finally, the focused beam was spread to the electron flux of below $4 \times 10^5$ A/m$^2$, yielding the specimen keeping aging in the gentle electron beam circumstance and the resulting structural evolution being monitored.

The HRTEM and HAADF-STEM experiments were performed in a Titan Cubed 60–300 kV aberration-corrected TEM fitted with a high-brightness field-emission gun (X-FEG) and double Cs corrector operating at 300 kV. The EELS spectra were acquired using Gatan Image Filter (GIF, Quantum 965) with the Dual-EELS acquisition

---

* Corresponding author.
*E-mail address:* bozhang@imr.ac.cn (B. Zhang).

http://dx.doi.org/10.1016/j.micron.2016.09.008

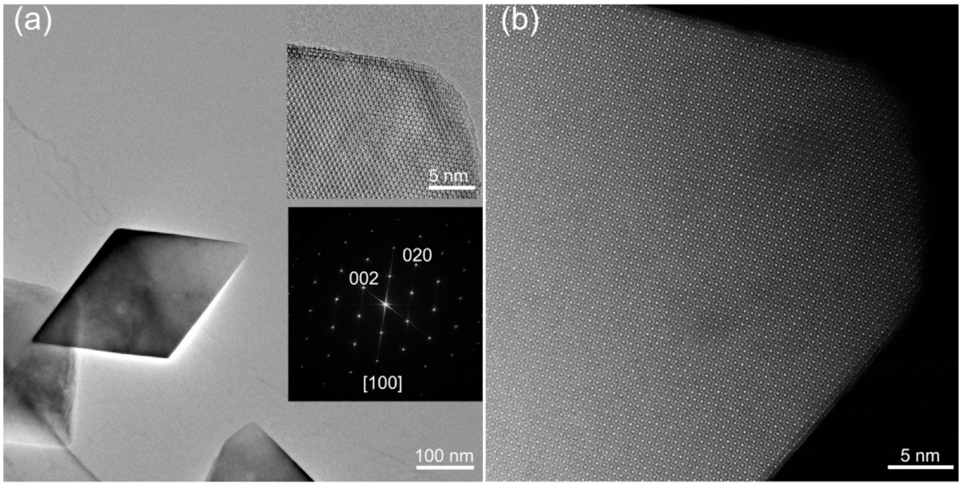

**Fig. 1.** Characterization on the as-synthesized $Mn_3O_4$ particles. (a) Low-magnification bright-field TEM image showing a typical rhombus shape of projection along [100] direction of a spinel octahedral-shape $Mn_3O_4$ nanoparticle. Insets are the HRTEM and the FFT images. (b) High resolution HAADF-STEM image along [100] zone axis showing the typical atom projection arrangement of spinel. It can be seen that the particle has the sharp and well-defined edge and the homogeneous structure from surface to interior.

mode. The probe convergence semi-angle was approximately 21.4 *m*rad. An energy dispersion of 0.25 eV/channel and 0.1 eV/channel was used and the energy resolution of the system was roughly 1.8 eV and 1.2 eV, respectively. In order to avoid adopting the unreliable signals induced by the contingent beam damage during the EELS experiments, we acquired and compared the two images from the same region before and after scanning to ensure free of damage.

## 3. Results and discussion

### 3.1. The structure evolution induced by the electron irradiation

Fig. 1a is a low-magnification TEM image, showing the nano-sized $Mn_3O_4$ particle has a well-defined octahedral shape. The HRTEM image (Fig. 1a, inset) and the HAADF-STEM image (Fig. 1b) along the [100] direction show the perfectly sharp edge, and the Fast Fourier transform (FFT) (Fig. 1a, inset) of the HRTEM image can be indexed to be the tetragonal $Mn_3O_4$ structure with the space group $I4_1/amd$. The $Mn_3O_4$ TEM specimen was irradiated by a focused electron beam with a constant current density of about $9 \times 10^5$ A/m$^2$ for some duration and then was tracked the irradiation induced structural evolution. The high resolution HAADF-STEM image is shown in Fig. 2a and the zoom-in image is shown in Fig. 2b. The [100] crystal direction is frequently chosen because the $Mn^{2+}$ (in Purple) and $Mn^{3+}$ (in Green) cations are separated in different atomic columns, and the $Mn^{2+}$ atoms are located at the 8a tetrahedral sites in the lattice while the $Mn^{3+}$ atoms are located on the 16d octahedral site (Tan et al., 2011). It is evident that the rocksalt structure was nucleated at the edge of the $Mn_3O_4$, which indicates that electron beam induces the transformation of spinel $Mn_3O_4$ to rocksalt structure yielding the formation of the reconstruction skin layer. Interestingly, in-situ HRTEM experiment was recorded in video 1 in the Supplementary material, which clearly shows the evolution process of crystal structure. The orientation relationship is rocksalt structure [110]//$Mn_3O_4$ [100] and rocksalt structure (-110)//$Mn_3O_4$ (010), as indicated in the FFT inset. Fig. 2c shows the EELS full spectra, which were obtained from the bulk and the reconstruction region respectively. Fig. 2d shows the enlarged view of the O-K edge, where the prepeak structure of the O-K edge can be interpreted in terms of transition processes governed by the dipole selection rule (Kurata and Colliex, 1993). Fig. 2e shows the enlarged view covering the Mn-$L_{2,3}$ edges. Compared with the bulk, the Mn-$L_2$ and $L_3$ edges corresponding to the reconstruction region are found to shift towards the lower energy loss, which indicates the decrease in the average oxidation state of transition metal cations at the surface. Besides that, with the method of double arctangent and the Pearson method (Van Aken et al., 1998; Pearson et al., 1993; Wang et al., 2000; Tan et al., 2012), the white-line intensity ratio $I(L_3)/I(L_2)$ for the bulk and the surface is calculated to be roughly 2.8 and 3.6, respectively. The higher $I(L_3)/I(L_2)$ ratio is another indicator of a lower valance on the surface transformed layer. The lower oxidation state of manganese should be bivalent manganese and thus the rocksalt structured reconstruction layer is identified to be MnO.

It is noteworthy that people usually focus on the decomposition and reduction from the high oxidation states to low oxidation states for transition metal oxides. For examples, $V_2O_5$, $TiO_2$, $MoO_3$ and $Nb_2O_5$ would transform to rocksalt structure suboxides by electron irradiation (Su and Schlögl, 2002; Wang et al., 2004; Smith et al., 1987; Xu et al., 1993). The damage induced by irradiation usually is believed to be an irreversible process (Pennycook et al., 2014). Interestingly, by aging, we observed that the transformed rocksalt structured MnO can recover to the original spinel structured $Mn_3O_4$ and thus concluded that the damage indeed is a reversible process. After irradiating the specimen for some duration, the electron beam was spread and thus the specimen was aged in the friendly gentle beam circumstance. Then we monitored the structure evolution.

Fig. 3a is the HAADF image showing the evolution of the rocksalt structured transformed layer after aging for about 5 min. The observed region is the same place with that shown in Fig. 2a. It is seen that a very small region at the outmost surface has recovered to the spinel structure as marked with white circle. Further aging for half an hour, the transformed region has almost recovered to the spinel structure except a very small middle zone keeping rocksalt structure as marked with red circle in Fig. 3b. This is in accordance with the in-situ HRTEM observation recorded in the simplified video 2 in the Supplementary material. It is shown that the recover process goes from outside to inside. The enlarged view of the sandwich-like region is shown in Fig. 3c, where three regions marked with the white circles are chosen to perform the EELS analysis and the spectra are shown in Fig. 3d. Since the material is quite electron beam sensitive, relatively low doses and quick acquirement time are necessary. Compared with the spectra of the bulk region 1, the evident chemical shift, as expected, is clearly observed in the region 2, and doesn't occur in the recovered region 3. Evi-